



EXPERIMENTAL INVESTIGATIONS OF THE  
INFLUENCE OF REYNOLDS NUMBER AND  
BOUNDARY CONDITIONS ON A PLANE AIR JET

BY

RAVINESH C. DEO

MSC HONS (*Canterbury*): BSc (*USP*)

A THESIS SUBMITTED IN FULFILLMENT OF THE  
REQUIREMENTS FOR THE DEGREE OF  
DOCTOR OF PHILOSOPHY

IN

ENGINEERING

AT

TURBULENCE, ENERGY AND COMBUSTION GROUP  
SCHOOL OF MECHANICAL ENGINEERING  
THE UNIVERSITY OF ADELAIDE  
SOUTH AUSTRALIA SA 5005

SEPTEMBER 30, 2005

# Experimental Investigations of the Influence of Reynolds Number and Boundary Conditions on a Plane Air Jet

RAVINESH C DEO

JUNE 07, 2005 THESIS SUBMITTED

OCTOBER 07, 2005 DEGREE AWARDED

Thesis for Doctor of Philosophy in Engineering

Supervisors: Assoc. Professor G J Nathan

Senior Research Fellow Dr. J Mi

## ORIGINALITY STATEMENT

I, Ravinesh C. DEO, hereby declare that this thesis, titled “Experimental Investigations of the Influence of Reynolds Number and Boundary Conditions on a Plane Air Jet”, submitted for the award of a Doctor of Philosophy in Engineering at The University of Adelaide, is original in every respect. It contains no material which has been accepted for the award of any other degree or diploma in any university. Further to the best of my knowledge and belief, this Ph.D. thesis contains no material previously published or written by another person, except where due reference is made in the thesis.

---

Ravinesh C. DEO

---

date

## COPYING PERMISSION

In presenting the fulfillment of the requirements for the degree of Doctor of Philosophy in Engineering at The University of Adelaide, I agree that the Library shall make it freely available for inspection and copying under the Copyright Law of Australia. It is understood that any copying or publication of this Ph.D. research for financial gain shall not be allowed without my written permission. I hereby grant permission to the library at The University of Adelaide to photocopy my work for scholarly purposes only.

---

Ravinesh C. DEO

---

date

# Contents

|  |             |
|--|-------------|
| <b>Tables</b>  | <b>v</b>    |
| <b>Figures</b>   | <b>vi</b>   |
| <b>Abstract</b>  | <b>xiii</b> |
| <b>Acknowledgements</b>  | <b>xvii</b> |
| <b>Nomenclature</b>  | <b>xxi</b>  |
| 0.1 Acronyms . . . . .   | xxi         |
| 0.2 Greek Symbols . . . . .  | xxiii       |
| 0.3 Some Special Terms . . . . .   | xxiii       |
| 0.4 Coordinate System . . . . .  | xxiii       |
| <b>1 INTRODUCTION</b>  | <b>2</b>    |
| 1.1 Introductory Note . . . . .  | 2           |
| 1.2 History of Plane Jets . . . . .  | 3           |
| 1.3 Characteristics of a Plane Jet . . . . .                                   | 4           |
| 1.4 Definitions of Initial and Boundary Conditions . . . . .                   | 6           |
| 1.4.1 Reynolds Number of a Plane Jet . . . . .                                 | 6           |
| 1.4.2 Nozzle Aspect Ratio of a Plane Jet . . . . .                             | 7           |
| 1.4.3 Nozzle Geometry and Inner-Wall Nozzle Exit Contraction Profile . . . . . | 7           |
| 1.4.4 Sidewalls in a Plane Jet . . . . .                                       | 9           |
| 1.5 Literature Review . . . . .  | 9           |
| 1.5.1 Influence of Jet Exit Reynolds Number . . . . .                          | 10          |
| 1.5.2 Effect of Inner-Wall Nozzle Exit Contraction Profile . . . . .           | 15          |
| 1.5.3 Effect of Nozzle Aspect Ratio on Rectangular and Plane Jets . . . . .    | 21          |
| 1.5.4 Sidewalls in a Plane Jet . . . . .                                       | 26          |
| 1.6 Motivation for Present Work . . . . .                                      | 29          |
| 1.7 Thesis Objectives . . . . .  | 30          |

|          |   |           |
|----------|---|-----------|
| 1.8      | Thesis Outline . . . . .  | 31        |
| <b>2</b> | <b>EXPERIMENTATION</b>  | <b>34</b> |
| 2.1      | Wind Tunnel Facility . . . . .                                    | 34        |
| 2.2      | Plane Nozzle Facility . . . . .                                   | 35        |
| 2.3      | Assessment of Effects of Room Confinement . . . . .               | 37        |
| 2.3.1    | Experimental Facility Parameters . . . . .                        | 38        |
| 2.3.2    | Loss of Axial Momentum . . . . .                                  | 39        |
| 2.3.3    | Similarity of the Mean Velocity Field for the Plane Jet . . . . . | 39        |
| 2.4      | Hot Wire Anemometry . . . . .                                     | 40        |
| 2.4.1    | Historical Aspects . . . . .                                      | 41        |
| 2.4.2    | Advantages and Disadvantages . . . . .                            | 41        |
| 2.4.3    | Hot Wire Probes . . . . .   | 45        |
| 2.4.4    | CTA Circuit . . . . .   | 45        |
| 2.4.5    | The Present Hot-Wire Configurations . . . . .                     | 49        |
| 2.4.6    | Hot Wire Calibration . . . . .                                    | 50        |
| 2.5      | Data Acquisition . . . . .  | 51        |
| 2.6      | Experimental Uncertainties . . . . .                              | 51        |
| 2.6.1    | Calibration Error . . . . .                                       | 52        |
| 2.6.2    | Data Acquisition System Error . . . . .                           | 53        |
| 2.6.3    | Other Uncertainties . . . . .                                     | 54        |
| 2.6.4    | Summary of Errors . . . . .                                       | 54        |
| 2.7      | Summary of Experimental Conditions . . . . .                      | 56        |
| <b>3</b> | <b>INFLUENCE OF REYNOLDS NUMBER</b>                               | <b>58</b> |
| 3.1      | Introduction . . . . .  | 58        |
| 3.2      | Experiment Details . . . . .                                      | 59        |
| 3.3      | Results and Discussion . . . . .                                  | 61        |
| 3.3.1    | The Initial Velocity Field . . . . .                              | 61        |
| 3.3.2    | The Mean Velocity Field . . . . .                                 | 64        |
| 3.3.3    | The Fluctuating Velocity Field . . . . .                          | 71        |
| 3.4      | Further Discussion . . . . .                                      | 85        |
| 3.5      | Conclusions . . . . .   | 94        |
| <b>4</b> | <b>EFFECT OF INNER-WALL NOZZLE EXIT CONTRACTION PRO-<br/>FILE</b> | <b>97</b> |
| 4.1      | Introduction . . . . .  | 97        |

|          |  |            |
|----------|--|------------|
| 4.2      | Experiment Details . . . . .             | 98         |
| 4.3      | Results and Discussion . . . . .         | 99         |
| 4.3.1    | The Initial Velocity Field . . . . .     | 99         |
| 4.3.2    | The Mean Velocity Field . . . . .        | 103        |
| 4.3.3    | The Fluctuating Velocity Field . . . . . | 110        |
| 4.4      | Further Discussion . . . . .             | 115        |
| 4.5      | Conclusions . . . . .                    | 126        |
| <b>5</b> | <b>EFFECT OF NOZZLE ASPECT RATIO</b>     | <b>129</b> |
| 5.1      | Introduction . . . . .                   | 129        |
| 5.2      | Experiment Details . . . . .             | 130        |
| 5.3      | Results and Discussion . . . . .         | 131        |
| 5.3.1    | The Initial Velocity Field . . . . .     | 131        |
| 5.3.2    | The Mean Velocity Field . . . . .        | 134        |
| 5.3.3    | The Fluctuating Velocity Field . . . . . | 144        |
| 5.4      | Further Discussion . . . . .             | 150        |
| 5.5      | Conclusions . . . . .                    | 156        |
| <b>6</b> | <b>EFFECT OF SIDEWALLS</b>               | <b>159</b> |
| 6.1      | Introduction . . . . .                   | 159        |
| 6.2      | Experiment Details . . . . .             | 160        |
| 6.3      | Results and Discussion . . . . .         | 160        |
| 6.3.1    | The Mean Velocity Field . . . . .        | 160        |
| 6.3.2    | The Fluctuating Velocity Field . . . . . | 165        |
| 6.4      | Further Discussion . . . . .             | 170        |
| 6.5      | Conclusions . . . . .                    | 175        |
| <b>7</b> | <b>CONCLUSIONS</b>                       | <b>177</b> |
| <b>A</b> | <b>THESIS ASSESSMENT DETAILS</b>         | <b>183</b> |
| A.1      | Examination Documents . . . . .          | 183        |
| A.2      | Examiners Reports . . . . .              | 183        |
| <b>B</b> | <b>PUBLICATIONS FROM THIS WORK</b>       | <b>184</b> |
| <b>C</b> | <b>PREPRINT OF PUBLICATIONS</b>          | <b>186</b> |

|          |   |            |
|----------|---|------------|
| <b>D</b> | <b>MATLAB PROGRAMS</b>  | <b>187</b> |
| D.1      | General Data Reading and Writing . . . . .                                | 187        |
| D.2      | Skewness and Flatness Factors . . . . .                                   | 189        |
| D.3      | PDF and Power Spectrums . . . . .   | 191        |
| D.4      | Filtering Routines for Real-time Instantaneous Velocity Signals . . . . . | 193        |
| <b>E</b> | <b>DERIVATIONS, CONCEPTS AND SUPPLEMENTARY RESULTS</b>                    | <b>194</b> |
| E.1      | Derivation of Axial Loss in Momentum for Plane Jet . . . . .              | 194        |
| E.2      | Derivation of Bulk Mean Velocity from Initial Velocity Profiles . . . . . | 195        |
| E.3      | General Formulation of Reynolds Number . . . . .                          | 197        |
| E.4      | Re-Effect on Axial Distribution of Strouhal Numbers . . . . .             | 198        |
| E.5      | Preliminary Assessment of Nozzle Exit Contraction Profile . . . . .       | 199        |
| E.6      | Different Normalizations of Centerline Mean Velocity . . . . .            | 200        |
| E.7      | More Discussion on Initial Conditions . . . . .                           | 201        |
| <b>F</b> | <b>Heat Transfer Principles Relevant to Hot Wire Anemometry</b>           | <b>203</b> |
|          | <b>Bibliography</b>   | <b>205</b> |

# List of Tables

|     |   |     |
|-----|---|-----|
| 2.1 | Contributions of errors to the mean and turbulent statistics from different sources. . . . .  | 55  |
| 2.2 | Errors in the mean and turbulent quantities. . . . .  | 55  |
| 2.3 | Actual errors in jet properties. . . . .  | 55  |
| 2.4 | A summary of the initial conditions of each experiment, from Chapters 3-6.  | 57  |
| 3.1 | Summary of the pseudo-boundary-layer characteristics (mm) of the plane jet at different Reynolds numbers of investigation. . . . .  | 62  |
| 3.2 | A literature summary of the centerline mean velocity decay and spreading rates of a plane jet. . . . .  | 73  |
| 4.1 | Summary of the pseudo-boundary-layer characteristics (mm) of the plane jet for different inner-wall nozzle contraction profiles, $r^*$ . . . . .  | 102 |
| 4.2 | The normalized vortex shedding frequency $St$ for previous round, rectangular and plane jets. Note Sato (1960) <sup>3</sup> : used a planar nozzle, but at the nozzle with an upstream channel of length between 300-1100 mm. . . . . | 119 |
| 5.1 | Summary of the pseudo-boundary-layer characteristics (mm) of the plane jet for different nozzle aspect ratios. . . . .  | 133 |



# List of Figures

|      |   |      |
|------|---|------|
| 1    | The coordinate system used in the present study. . . . .  | xxiv |
| 1.1  | A schematic view of a plane jet nozzle. . . . .   | 5    |
| 1.2  | A schematic view of the time-averaged flow field of a plane jet. . . . .  | 6    |
| 1.3  | The nozzle aspect ratio, defined by $AR = w/H$ for a plane jet of nozzle dimensions $w \times H$ . . . . .  | 7    |
| 1.4  | A schematic view of (a) a smooth contraction (b) a sharp-edged and (c) a radially contoured rectangular nozzle. . . . .   | 8    |
| 1.5  | Laser-induced fluorescence streak images of the scalar field in a liquid-phase shear layer for (a) $Re = 1.75 \times 10^3$ and (b) $Re = 2.30 \times 10^4$ . . . . .  | 11   |
| 1.6  | Summary of previous measurements of Reynolds number effect on the centerline turbulence intensity of a plane jet. Note: HC77 - Hussain and Clark (1977), GW76 - Gutmark and Wygnanski (1976), B67 - Bradbury (1965), H65 - Heskestad (1965), BARC82 - Browne <i>et al.</i> (1982), NO88 - Namar and Ötügen (1988) and TG86 - Thomas and Goldschmidt (1986). . . . . | 13   |
| 1.7  | A schematic view of a smooth contraction plane nozzle used by Antonia <i>et al.</i> (1982), Thomas and Goldschmidt (1986) and Gutmark and Wygnanski (1976). . . . .   | 16   |
| 1.8  | A long pipe nozzle $L \gg D$ as used by Antonia and Zhao (2001), Mi <i>et al.</i> (2001) and Mi and Nathan (2004). . . . .  | 17   |
| 1.9  | Initial velocity profiles from a sharp-edged orifice nozzle, a smooth contraction nozzle and a long pipe for a round jet. . . . .   | 18   |
| 1.10 | A schematic view of the sharp-edged orifice nozzle used by Heskestad (1965). . . . .  | 19   |
| 1.11 | The orifice plate used by Quinn (1992a) . . . . .   | 20   |
| 1.12 | The round nozzle used by Klein and Ramjee (1972) and Ramjee and Hussain (1976). Note that the nozzle contraction ratio is the ratio of $D_i$ and $D_e$ . . . . .  | 20   |
| 1.13 | The range of data sets of previous measurements of the mean velocity decay of a plane jet at various nozzle aspect ratios. Here, BO75 refers to Bashir and Uberio (1975), H65: Heskestad (1965), H90: Hitchman <i>et al.</i> (1965), TG86: Thomas and Goldschmidt (1986), MC57: Miller and Commings (1957) and B84: Browne <i>et al.</i> (1984). . . . .            | 22   |

|      |   |    |
|------|---|----|
| 1.14 | The growth of boundary layer due to a flow past a wall. Modified after Frank (1999). . . . .  | 24 |
| 1.15 | A summary of previous measurements of the turbulence intensity of plane jet investigations, at different nozzle aspect ratios. Note: Symbols identical to Figure 1.13. . . . .                                    | 26 |
| 1.16 | A schematic view of the smooth contraction (round) nozzle, (a) with and (b) without, front plates. . . . .  | 27 |
| 1.17 | A model of the entrainment into a radially contoured plane jet (a) with and (b) without sidewalls. . . . .  | 29 |
| 2.1  | The overall experimental arrangement showing the nozzle attachment to the wind tunnel, hot wire probes, connections, anemometer and data acquisition system. Note that sidewalls are omitted for clarity. . . . . | 35 |
| 2.2  | A schematic view of the present wind tunnel facility. . . . .   | 36 |
| 2.3  | A schematic view of (a) a standard smooth contraction and (b) a radial contraction nozzle. Note: $L/H \gg 60$ . . . . .   | 37 |
| 2.4  | A schematic view of the experimental laboratory. . . . .  | 39 |
| 2.5  | The CTA electronic circuit. . . . .   | 46 |
| 2.6  | The correct square wave test. . . . .   | 48 |
| 2.7  | A typical fourth-order polynomial curve for the calibration, before and after experiment. . . . .   | 52 |
| 3.1  | A schematic diagram of the plane jet facility, showing the wind tunnel, plane nozzle and sidewalls. . . . .   | 60 |
| 3.2  | Lateral profiles of (a) the normalized mean velocity $U_n$ and (b) the turbulence intensity $u'_n$ obtained at $x/H \simeq 0.5$ for $1,500 \leq Re \leq 16,500$ . . . . .   | 61 |
| 3.3  | The centerline variation of the near field mean velocity $U_c/U_{o,c}$ and the potential core length $x_p$ at different Reynolds number $Re$ . . . . .  | 65 |
| 3.4  | Lateral profiles of the mean velocity $U/U_c$ at $x/H = 5$ . . . . .  | 66 |
| 3.5  | The centerline variation of the normalized mean velocity $(U_{o,c}/U_c)^2$ for different Reynolds number $Re$ . Note: H90 - Hitchman (1990), JG73 - Jenkins and Goldschmidt (1973). . . . .                       | 67 |
| 3.6  | Dependence of the centerline decay rate of mean velocity $K_u$ and the virtual origin $x_{01}$ on the Reynolds number $Re$ . . . . .  | 68 |
| 3.7  | Lateral profiles of the normalized mean velocity $U_n$ for $Re = 1,500$ . . . . .   | 69 |
| 3.8  | Lateral profiles of the normalized mean velocity $U_n$ for $Re = 3,000$ . . . . .   | 69 |
| 3.9  | Lateral profiles of the normalized mean velocity $U_n$ for $Re = 7,000$ . . . . .   | 70 |
| 3.10 | Lateral profiles of the normalized mean velocity $U_n$ for $Re = 10,000$ . . . . .  | 70 |
| 3.11 | Lateral profiles of the normalized mean velocity $U_n$ for $Re = 16,500$ . . . . .  | 71 |
| 3.12 | The streamwise variation of the velocity half-width $y_{0.5}$ at different Reynolds number $Re$ . . . . .   | 72 |
| 3.13 | Dependence of the jet spreading rate $K_y$ on the Reynolds number $Re$ . . . . .  | 74 |

|      |  |     |
|------|--|-----|
| 3.14 | Evolutions of the centerline turbulence intensity $u'_{n,c}$ for different Reynolds numbers $Re$ . . . . .   | 75  |
| 3.15 | Trace signal of the velocity fluctuations, $u$ at an axial location where turbulence intensity, $u'_{n,c} = u'_{c,max}$ for $Re = 1,500, 7,000$ and $16,500$ . . . . .   | 76  |
| 3.16 | Reynolds number $Re$ effect on the near field hump in turbulence intensity $u'_{c,max}$ and on the far field asymptotic turbulence intensity $u'_{c,\infty}$ . . . . .   | 76  |
| 3.17 | The variation of local Reynolds number, $Re_{local}$ with downstream distance, for different jet exit Reynolds numbers. . . . .  | 77  |
| 3.18 | The dependence of centerline turbulence intensity, $u'_{n,c}$ on the local Reynolds Number, $Re_{local}$ for different jet exit Reynolds numbers. . . . .  | 78  |
| 3.19 | Reynolds number $Re$ effect on the turbulent kinetic energy dissipation $\epsilon$ . . . . .   | 81  |
| 3.20 | Lateral profiles of the turbulence intensity $u'_n$ for $Re = 1,500$ . . . . .   | 82  |
| 3.21 | Lateral profiles of the turbulence intensity $u'_n$ for $Re = 3,000$ . . . . .   | 82  |
| 3.22 | Lateral profiles of the turbulence intensity $u'_n$ for $Re = 7,000$ . . . . .   | 83  |
| 3.23 | Lateral profiles of the the turbulence intensity $u'_n$ for $Re = 10,000$ . . . . .  | 83  |
| 3.24 | Lateral profiles of the the turbulence intensity $u'_n$ for $Re = 16,500$ . . . . .  | 84  |
| 3.25 | The Reynolds number $Re$ dependence of the centerline skewness factors $S_u$ up to $x/H = 160$ . . . . .   | 85  |
| 3.26 | The Reynolds number $Re$ dependence of the centerline flatness factor $F_u$ . . . . .  | 86  |
| 3.27 | Dependence of the far field asymptotic skewness $S_u^{c,\infty}$ and the far field asymptotic flatness $F_u^{c,\infty}$ , on Reynolds number, $Re$ . . . . .   | 87  |
| 3.28 | The dependence of the centerline decay rate $K_u$ of the mean velocity on Reynolds number $Re$ in the jet of Lemieux and Oosthuizen (1985). . . . .  | 88  |
| 3.29 | Power spectra $\phi_u$ of the centerline velocity fluctuations $u$ at $x/H = 4$ . . . . .  | 89  |
| 3.30 | A simplified view of the coherent structures in a turbulent plane jet. . . . .   | 90  |
| 3.31 | Laser Tomographic photographs of a quasi-plane jet measured over the axial range $0 \leq x/H \leq 60$ and Reynolds numbers over the range $90 \leq Re \leq 5,100$ . . . . .  | 91  |
| 3.32 | Flow visualization images of jet fluid concentration in the plane of symmetry of a turbulent round jet at: (a) $Re \simeq 2.5 \times 10^3$ and (b) $Re \simeq 10^4$ . . . . .  | 92  |
| 3.33 | Schlieren photograph of a quasi-plane jet measured over the axial range $25 \leq x/H \leq 45$ and Reynolds numbers over the range $260 \leq Re \leq 2,510$ . . . . .   | 93  |
| 4.1  | Nozzle plates used for inner-wall nozzle profile variation for the cases in (a) $4.5 \leq r^* \leq 36$ mm with radial contraction facing upstream and (b) radial contraction facing downstream i.e. $r^* \sim 0$ . . . . . | 98  |
| 4.2  | Lateral profiles of (a) the normalized mean velocity $U_n$ and (b) the turbulence intensity $u'_n$ at the $x/H \simeq 0.25$ for $0.45 \leq r^* \leq 3.60$ and $x/H = 1.25$ for $r^* \simeq 0$ . . . . .                    | 100 |

|      |  |     |
|------|--|-----|
| 4.3  | Variation of the exit centerline mean velocity $U_{o,c}$ relative to the bulk mean velocity $U_{o,b}$ for different $r^*$ , calculated from initial velocity profiles obtained at $x/H \simeq 0.25$ . . . . .  | 101 |
| 4.4  | The calculated boundary thickness (mm) obtained at $x/H \simeq 0.25$ and translated to $x/H \simeq 0$ to provide a pseudo-exit boundary layer thickness (mm) $\delta$ for different inner-wall nozzle contraction profiles $r^*$ . . . . .   | 103 |
| 4.5  | Near field evolution of the normalized mean centerline velocity $U_{n,c}$ on the nozzle contraction profile factor $r^*$ . . . . .   | 104 |
| 4.6  | The dependence of the ratio of the centerline mean velocity maximum $U_{m,c}$ to the exit centerline mean velocity $U_{o,c}$ (i.e. $U_{m,c}/U_{o,c}$ ) on the nozzle contraction profile factor $r^*$ at $x/H \simeq 3$ . . . . .  | 105 |
| 4.7  | The far field centerline mean velocity in the inverse square form, normalized using the bulk mean velocity $U_{o,b}$ for different nozzle profiles $r^*$ . . . . .   | 107 |
| 4.8  | Dependence of the centerline decay rate of mean velocity $K_u$ and the virtual origin $x_{01}$ on the nozzle contraction profile factor $r^*$ . . . . .  | 108 |
| 4.9  | Lateral profiles of the normalized mean velocity $U_n$ . (a) $r^* \simeq 0$ (b) $r^* \simeq 0.45$ and (c) $r^* = 3.60$ . . . . .   | 109 |
| 4.10 | The streamwise variation of the velocity half-width $y_{0.5}$ for different nozzle contraction profile factors $r^*$ . . . . .   | 110 |
| 4.11 | Dependence of the jet spreading rate $K_y$ and virtual origin $x_{02}/H$ on the nozzle contraction profile factor $r^*$ . . . . .  | 111 |
| 4.12 | Evolutions of the centerline turbulence intensity $u'_{n,c}$ for different nozzle contraction profile factor $r^*$ . . . . .   | 112 |
| 4.13 | Dependence of the far field asymptotic turbulence intensity $u'_{c,\infty}$ on the nozzle contraction profile factor $r^*$ . . . . .   | 113 |
| 4.14 | Lateral profiles of the turbulence intensity $u'_n$ for (a) $r^* \simeq 0$ (b) $r^* \simeq 0.45$ and (c) $r^* = 3.60$ . . . . .  | 114 |
| 4.15 | The nozzle profile dependence of the centerline skewness $S_u$ factors. . . . .  | 116 |
| 4.16 | The nozzle profile dependence of the centerline flatness, $F_u$ factors. . . . .   | 117 |
| 4.17 | Instantaneous planar images of the scalar fields of jets issuing from (a) a (round) smooth contraction and (b) a sharp-edged round nozzle. . . . .   | 118 |
| 4.18 | Schematic views of the sharp-edged nozzle profiles used by (a) Tsuchiya et al. (1989) for their rectangular nozzle (b) Beavers and Wilson (1970) for their plane nozzle (c) Sato (1960) for their plane nozzle with a channel of length $l$ at the exit (d) present investigation. . . . . | 120 |
| 4.19 | Power spectrum $\phi_u$ of the centerline velocity fluctuations $u$ at $x/H = 3$ . . . . .   | 121 |

|      |  |     |
|------|--|-----|
| 4.20 | The normalized vortex shedding frequency $St_H$ , calculated at $x/H = 3$ . Included are: the previous data obtained from a profile with a sharp-edged orifice measured by Tsuchiya et al. (1989) for their rectangular nozzle, Beavers and Wilson (1970) for their plane nozzle and Sato (1960) for his plane nozzle with an upstream channel of length $l$ ; and Namar and Ötügen obtained from their smoothly contoured quasi-plane nozzle. . . . . | 122 |
| 4.21 | Entrainment by (a) a radially contoured nozzle (with front plate) and (b) a smoothly contoured nozzle (without front plate). . . . .   | 125 |
| 4.22 | A plane nozzle (a) with front plate at the exit plane and (b) without front plate. . . . .   | 126 |
| 5.1  | A schematic view of the experimental setup for (a) $AR = 72$ and (b) $AR = 15$ . . . . .   | 131 |
| 5.2  | Lateral profiles of (a) normalized mean velocity $U_n$ and (b) the turbulence intensity $u'_n$ at $x/H = 0.25$ for different nozzle aspect ratios $AR$ . . . . .   | 132 |
| 5.3  | Pseudo-boundary layer thickness $\delta$ at $x = 0.25H$ computed from the initial velocity profiles. . . . .   | 134 |
| 5.4  | The near field centerline velocity variation $U_c/U_{o,c}$ , for different nozzle aspect ratios $AR$ and the corresponding potential core lengths $x_p$ . . . . .  | 135 |
| 5.5  | Lateral profiles of $U/U_c$ at $x/H = 3$ . . . . .   | 136 |
| 5.6  | Centerline variations of normalized mean velocity $U_{n,c}$ up to $x/H = 45$ . . . . .   | 137 |
| 5.7  | Dependence of the centerline decay rate of mean velocity $K_u$ obtained for $x/H > 20$ on the nozzle aspect ratio $AR$ . . . . .   | 138 |
| 5.8  | The centerline variation of the normalized mean velocity $(U_{o,c}/U_c)^2$ in the inverse square form, for different nozzle aspect ratio $AR$ up to $x/H = 90$ . . . . .   | 139 |
| 5.9  | The planar region $x_{p, \max}/H$ of the jet, at different nozzle aspect ratios $AR$ . . . . .   | 140 |
| 5.10 | Lateral profiles of the normalized mean velocity $U_n$ for $AR = 15$ . . . . .   | 141 |
| 5.11 | Lateral profiles of the normalized mean velocity $U_n$ for $AR = 20$ . . . . .   | 141 |
| 5.12 | Lateral profiles of the normalized mean velocity $U_n$ for $AR = 30$ . . . . .   | 142 |
| 5.13 | Lateral profiles of the normalized mean velocity $U_n$ for $AR = 50$ . . . . .   | 142 |
| 5.14 | Lateral profiles of the normalized mean velocity $U_n$ for $AR = 72$ . . . . .   | 143 |
| 5.15 | The streamwise variation of the velocity half-width $y_{0.5}$ for different nozzle aspect ratios $AR$ . . . . .  | 144 |
| 5.16 | Dependence of the jet spreading rate $K_y$ on the nozzle aspect ratio $AR$ . . . . .   | 145 |
| 5.17 | Dependence of the virtual origin $x_{02}/H$ on the nozzle aspect ratio $AR$ . A quadratic best-fit curve with its regression coefficient is shown. . . . .   | 146 |
| 5.18 | Dependence of the critical jet aspect ratio $AR_{jet,crit}$ at which the flow ceases to be planar, on the nozzle aspect ratio $AR$ . . . . .   | 147 |
| 5.19 | Evolutions of the centerline turbulence intensity $u'_{n,c}$ for different aspect ratios $AR$ . . . . .  | 148 |

|      |   |     |
|------|---|-----|
| 5.20 | Nozzle aspect ratio $AR$ effect on the near field hump in turbulence intensity $u'_{c,max}$ and on the far field asymptotic turbulence intensity $u'_{c,\infty}$ . A quadratic best-fit with its regression coefficient is shown. . . . . | 149 |
| 5.21 | Lateral profiles of the turbulence intensity $u'_n$ for $AR = 15$ . . . . .   | 150 |
| 5.22 | Lateral profiles of the turbulence intensity $u'_n$ for $AR = 20$ . . . . .   | 150 |
| 5.23 | Lateral profiles of the turbulence intensity $u'_n$ for $AR = 30$ . . . . .   | 151 |
| 5.24 | Lateral profiles of the turbulence intensity $u'_n$ or $AR = 50$ . . . . .  | 151 |
| 5.25 | Lateral profiles of the turbulence intensity $u'_n$ for $AR = 72$ . . . . .   | 152 |
| 5.26 | Centerline variations of the skewness factors $S_u$ . . . . .   | 153 |
| 5.27 | The minima $ S_u^{\min} $ and far field asymptotic value $S_u^\infty$ of skewness factors. . . . .  | 154 |
| 5.28 | The nozzle aspect ratio effect on the centerline flatness $F_u$ factors. The insert shows the near field maximum values of $F_u$ . . . . .  | 155 |
| 6.1  | The centerline mean velocity variation $U_{o,c}/U_c$ for a free rectangular jet (without sidewalls) and a plane jet (with sidewalls) on a logarithmic scale. The data of Quinn (1992a) for his free rectangular jet is shown. . . . .     | 162 |
| 6.2  | The centerline variation of the normalized mean velocity $(U_{o,c}/U_c)^2$ in the inverse square form for the free rectangular and plane jet. . . . .   | 163 |
| 6.3  | The streamwise variation of the velocity half-width $y_{0.5}$ for the free rectangular and plane jet. . . . .   | 165 |
| 6.4  | Evolutions of the centerline turbulence intensity $u'_{n,c}$ for free rectangular and plane jet. The inserted figure shows the close-up view for the near field. . . . .  | 167 |
| 6.5  | Power spectra $\phi_u$ of the centerline velocity fluctuations $u$ at $x/H \simeq 3$ showing the normalized vortex shedding frequency. . . . .  | 168 |
| 6.6  | The sidewall effect on the centerline skewness $S_u$ and the centerline flatness $F_u$ factors. . . . .   | 169 |
| 6.7  | Side and top views of the typical flow field of (a) a free rectangular jet and (b) a plane jet. . . . .   | 171 |
| 6.8  | A schematic view of (a) counter-rotating streamwise vortices in a plane jet (b) primary ring-like vortices in a free rectangular jet. . . . .   | 172 |
| 6.9  | Visualizations of ring-like vortices in a free rectangular (rectangular) jet. . . . .   | 173 |
| E.1  | The plane nozzle exit geometry, with dimensions and the initial velocity profile at $x/H = 0$ . . . . .   | 196 |
| E.2  | Lateral profiles of (a) the normalized mean velocity, $U_n$ (b) the turbulence intensity, $u'_n$ at $x = 0.5H$ for a sharp-edged orifice and a radially contoured nozzle, measured at $AR = 10$ and $60$ respectively. . . . .            | 198 |
| E.3  | Dependence of $St_H$ and $x/H$ for different Reynolds numbers. . . . .  | 199 |
| E.4  | Near field evolution of the normalized mean centerline velocity, $U_{n,c}$ (normalized using the bulk-mean velocity $U_{o,b}$ ) on the nozzle contraction profile factor, $r^*$ . . . . .   | 200 |

|     |  |     |
|-----|--|-----|
| E.5 | The far field centreline mean velocity in the inverse square form, normalized using the exit centerline mean velocity $U_{o,c}$ for different nozzle profiles. . . | 201 |
| E.6 | Variation of jet mass flow with downstream distance, showing the effect of jet entrainment. . . . .  | 202 |

# Abstract

A plane jet is a statistically two-dimensional flow, with the dominant flow in the stream-wise ( $x$ ) direction, spread in the lateral ( $y$ ) direction and zero entrainment in the spanwise ( $z$ ) direction respectively (see Figure 1). A plane jet has several industrial applications, mostly in engineering environments, although seldom is a jet issuing through a smooth contoured nozzle encountered in real life. Notably, the Reynolds number and boundary conditions between industrial and laboratory environments are different. In view of these, it is important to establish effects of nozzle boundary conditions as well as the influence of Reynolds number, on jet development. Such establishments are essential to gain an insight into their mixing field, particularly relevant to engineering applications. To satisfy this need, this thesis examines the influence of boundary conditions, especially those associated with the formation of the jet and jet exit Reynolds number, on the flow field of a turbulent plane air jet by measuring velocity with a hot wire anemometer. A systematic variation is performed, of the Reynolds number  $Re$  over the range  $1,500 \leq Re \leq 16,500$ , the inner-wall nozzle contraction profile  $r^*$  over the range  $0 \leq r^* \leq 3.60$  and nozzle aspect ratio  $AR$  over the range  $15 \leq AR \leq 72$  (see notation for symbols). An independent assessment of the effect of sidewalls on a plane jet is also performed. Key outcomes are as follows:

(1) *Effects of Reynolds number  $Re$*

Both the mean and turbulence fields show significant dependence on  $Re$ . The normalized initial mean velocity and turbulence intensity profiles are  $Re$ -dependent. An increase in the thickness of boundary layer at the nozzle lip with a decrease in  $Re$  is evident. This dependence appears to become negligible for  $Re \geq 10,000$ . The centerline mean velocity decay and jet spreading rates are found to decrease as  $Re$  is increased. Furthermore, the mean velocity field appears to remain sensitive to Reynolds number at  $Re = 16,500$ . Unlike the mean velocity field, the turbulent velocity field has a negligible  $Re$ -dependence for  $Re \geq 10,000$ . An increase in Reynolds number leads to an increase in the entrainment rate in the near field but a reduced rate in the far field. The centerline skewness and the flatness factors show a systematic dependence on Reynolds number too.



(2) *Effects of the inner-wall nozzle exit contraction profile  $r^*$*

The inner-wall nozzle exit contraction profile  $r^*$  influences the initial velocity and turbulence intensity profiles. Saddle-backed mean velocity profiles are evident for the sharp-edged orifice configuration ( $r^* \simeq 0$ ) and top hat profiles emerge when  $r^* \geq 1.80$ . As  $r^*$  is increased from 0 to 3.60, both the near and the far field decay and the spreading rates of the plane jet are found to decrease. Hence, the sharp-edged orifice-jet ( $r^* \simeq 0$ ) decays and spreads more rapidly than the jet through a radially contoured configuration ( $r^* \simeq 3.60$ ). The asymptotic values of the centerline turbulence intensity, skewness and flatness factors of the velocity fluctuations increase as  $r^*$  tends toward zero. The non-dimensional vortex shedding frequency of  $St_H \simeq 0.39$ , is higher for the sharp-edged orifice nozzle ( $r^* \simeq 0$ ), than for the radially contoured ( $r^* \simeq 3.60$ ) nozzle whose  $St_H \simeq 0.24$ . Thus, the vortex shedding should be strongly dependent on flow geometry and on nozzle boundary conditions.

(3) *Effects of nozzle aspect ratio  $AR$*

The initial velocity and turbulence intensity profiles are slightly dependent on nozzle aspect ratio of the plane air jet. It is believed that a coupled influence of the nozzle aspect ratio and sidewalls produce changes in the initial flow field. The axial extent over which a statistically ‘two-dimensional’ flow is achieved, is found to depend upon nozzle aspect ratio. This could be possibly due to the influence of the evolving boundary layer on the sidewalls or due to increased three-dimensionality, whose influence becomes significantly larger as nozzle aspect ratio is reduced. A statistically two dimensional flow is only achieved over a very limited extent for  $AR = 15$ . In the self-similar region, the rates of centreline velocity decay, spreading of the mean velocity field and jet entrainment increase with an increase in nozzle aspect ratio. An estimate of the ‘critical’ jet aspect ratio, where three-dimensional effects first emerge and its axial location is made. Results show that the critical aspect ratio increases with nozzle aspect ratio up to  $AR < 30$ . For  $AR \geq 30$ , the critical aspect ratio based on jet half width, attains a constant value of about 0.15. Thus, it appears that when the width of the flow approximately equals the spacing between the sidewalls, the plane air jet undergoes a transition from 2-D to 3-D. A distinct hump of the locally normalized turbulence intensity at an axial distance between 10 to 12 nozzle widths downstream, characterizes the centerline turbulence intensity for all nozzle aspect ratios. This hump is smaller when nozzle aspect ratio is larger.

(4) *Effects of the sidewalls*

A jet issuing from a nozzle of  $AR = 60$  and measured at  $Re = 7,000$  is tested with sidewalls, i.e. plane-jet and without sidewalls, i.e. free-rectangular-jet. It is found that the entire flow field behaves differently for the two cases. The initial velocity profiles are top hat for both jets. The free rectangular jet decays and spreads more rapidly in both the near and far field. It is found that the free rectangular jet behaves statistically two-dimensional up to a shorter axial distance ( $x/H = 70$ ) as opposed to the plane jet whose two-dimensional region extends up to  $x/H = 160$ . Also noted are that the axial extent of the two-dimensional region depends strongly on nozzle aspect ratio. Beyond the 2-D region, the free rectangular jet tends to behave, statistically, like a round jet. The locally normalized centerline turbulence intensity also depend on sidewalls. Turbulence intensity for the plane jet asymptotes closer to the nozzle (around  $x/H = 30$ ) whereas for the free rectangular jet, turbulence intensity varies as far downstream as  $x/H = 100$ , and then asymptotes. A constant  $St_H$  of 0.36 is found for the free rectangular jet whereas an  $St_H$  of 0.22 is obtained for the plane jet.

It is noted that the effects of jet exit Reynolds number, inner-wall nozzle exit contraction profile, nozzle aspect ratio and sidewalls on the plane air jet are all non-negligible. The effect of viscosity is expected to weaken with increased Reynolds number and this may contribute to the downstream effects on the velocity field. Both the nozzle contraction profile and nozzle aspect ratio provide different exit boundaries for the jet. Such boundary conditions not only govern the formation of the initial jet but also its downstream flow properties. Hence, the initial growth of the shear layers and the structures within these layers are likely to evolve differently with different boundary conditions. Thus, the interaction of the large-scale structures with the surroundings seems to depend on nozzle boundary conditions and consequently, influences the downstream flow. In summary, the present study supports the notion that the near and far fields of the plane jet are strongly dependent on Reynolds number and boundary conditions. Therefore, the present thesis contains immensely useful information that will be helpful for laboratory-based engineers in selection of appropriate nozzle configurations for industrial applications.



...Thankyou My Lord...

-----

To

**My Loving Parents**

**Amma & Daddy**

For Their Blessings & Inheritance

For The Achievement of my PhD

And

**My Dear Wife**

**Aruna**

For Her Love, Sacrifice & Encouragement

Towards my PhD

# Acknowledgements

Most sincere gratitude goes to my supervisors, Associate Professor Graham (Gus) Nathan and Dr. J Mi for their tremendous efforts in making this research a great success. Their contributions to my research degree, over the past  $3\frac{1}{2}$  years is immeasurable. I clearly understand that it is not possible for me to thank them by these few words. Evidence of their continued professional support, encouragement, guidance and friendship is revealed through the quality of my work, and every bit of it goes to them.

Since August 2001, Gus has been providing me tremendous support, not only in his capacity as my supervisor, but also as a close colleague and friend in working together towards the completion of this project. I also acknowledge him for providing me with the ARC Supplementary Scholarship and FCT short-term scholarship. My experimental skills are entirely dedicated to Dr. J Mi who not only taught me the techniques of hot-wire anemometry but also worked with me side-by-side everyday to assist me in solving problems that I encountered during my research. In the midst of 2003 when a significant event occurred that changed my wife and my life, Gus and Jamie were over-supportive and extremely cooperative with us. During this period, they provided me emotional support and guidance, so I thank them from my inner conscience. I must admit that Gus and J Mi are the best supervisors any postgraduate student can possibly have!

I acknowledge Dr. Peter Venon Lanspeary for acting as my co-supervisor in the initial stages of my Ph.D. His assistance in producing technical drawings of the nozzle designs are greatly appreciated. I would also like to thank Dr. Richard Kelso for few thoughtful discussions and George Osborne for designing hot-wire probes, Derek Franklin for setting up the traverse and Bill Finch / Bob Dyer for building my nozzles. Other workshop staff, in particular, Ron Jager and Malcom Bethune assisted me in setting up the plane jet facility. I acknowledge School of Mechanical Engineering for allowing me to pursue a Ph.D. in Engineering without having any prior engineering background. Acknowledgement is made to the school for funding my 15<sup>th</sup> AFMC conference. Thanks to the computer officer, Billy for his efforts in solving my PC problems!

My Ph.D. was supported by an International Postgraduate Research Scholarship (IPRS) and the Adelaide University Scholarship (AUS). Hence, I extend very special thanks to the Australian Government and Adelaide University for providing me funding. Acknowledgement is made to Australian Research Council (ARC) Discovery Grant for providing extra living allowances and incidental expenses towards the project. I thank the University of Adelaide for organizing the Intergrated Bridging Programme (IBP) for enhancing our skills in research and to Ms Karen Adams for her advice, guidance and interesting classes organized through the IBP.

On this landmark day, I acknowledge and remember three most important people in my life. Their contributions towards my Ph.D. are worthy of very special and humble thanks and remembrance. They are my loving **mum** and **dad** and my dear wife **Aruna**. My **parents, Mr and Mrs Bisun Deo**, deserve the highest level of respect for their benediction towards my achievement, endurance in educating me and for providing me the inheritance to be the first professional doctorate in our family. Indeed this Ph.D. is a dream they have visualized through me and I thank them for their sacrifice, prayers and blessings.

It is impossible for me to quantify the amount of support provided by my **wife, Aruna** on every stage of my career. Her words of encouragement, enthusiasm and advice still beeps in my ears, especially those which convinced me not to quit! The strength of her determination that I will be able to complete this huge task was a driving force behind my success. She sacrificed a large portion of her own career, luxury and indeed her invaluable time towards my doctorate. *It is to my parents and my wife that I dedicate my entire thesis.*

I would like to acknowledge my other parents (Mr and Mrs Chandar Deo) for providing heaps of blessings. In fact, mum deserves a lot of thanks for doing the cooking and housework when we were in desperate need! I wish to thank my brotherly friend Nilesh, for his inspirational discussions, his wife Neeliya for coming over to Adelaide to share my family load when we were in desperate need, and my close friend and colleague, Shakeel for being with us in this anonymous land, assisting me with some of my experimental setup and discussing with me my problems and progress regularly. I acknowledge my brothers (Rakesh, Pritam), sister (Madhu) + family members, relatives and friends whom I have not been able to include. Very special acknowledgment goes to well-known academics, Professor W K George (Chalmers University of Technology, Sweden) and Dr S Rajgopalan

(University of Newcastle, Australia) for providing a thoughtful and an excellent thesis review and commendations for this work.

Above all, thankyou my Lord for giving me the potentials for an extraordinary opportunity in my life. Your guidance has always been there, and without your will, nothing would have been possible!

© R C Deo

BSc (The University of the South Pacific Fiji)

MSc Hon (The University of Canterbury New Zealand)

SEPTEMBER 30, 2005 Email physcd@yahoo.com

## Vita

Born in a remote village of Naleba in the township of Labasa, Fiji Islands, Ravinesh gained his primary education at Naleba Bhartiya School from Classes 1-6 and junior secondary education at Naleba College from Forms 1-4. He undertook high school education from Forms 5-7 at Labasa College. He was the High School ‘Dux’ (Best High School academic student) in 1995, for achieving the highest standards in Mathematics, Biology, Chemistry and Physics. During this year, he broke the *Year 13 National Examination* (Fiji Seventh Form Examination) **ALL-TIME** record, by scoring the highest mark of 360/400 for the *first* time in the Fiji. His exam results created a new record of 97% in Physics and 96% in Chemistry.

Ravinesh completed his BSc in 1998, with subject majors, Physics and Mathematics from University of the South Pacific in Fiji. He was awarded the University Gold Medal and Motibhai Prize for being the outstanding Physics student. Overall, his GPA was at the High Distinction level (4.4/4.5). He continued for further education, to pursue an MSc in Meteorological Physics at University of Canterbury, New Zealand. He completed his masters successfully in May 2001, with degree awarded (with Honors) in July 2001. From August 2001 - April 2005, Ravinesh worked on his PhD project, within the Turbulence, Energy and Combustion [TEC] Group, School of Mechanical Engineering, University of Adelaide.

This doctoral dissertation was officially submitted on 07 June 2005. The Adelaide Graduate Center officially confirmed the award of a PhD (subject to minor amendments satisfactory to the supervisors) on 22 August 2005. Ravinesh now works as an Associate

Lecturer in Physics at University of the South Pacific in Fiji. His interest in fluid mechanics continues, and he hopes to pursue a post-doctoral, subject to career opportunity.

# Nomenclature

## 0.1 Acronyms

|                 |   |
|-----------------|---|
| $H$             | length of the short side of nozzle  |
| $w$             | length of the long side of the nozzle   |
| $r$             | contraction radius of the nozzle profile  |
| $AR$            | nozzle aspect ratio, where $AR = w/H$   |
| $r^*$           | contraction ratio of the nozzle profile, where $r^* = r/H$                                  |
| $l_w$           | length of the hot-wire sensor   |
| $d_w$           | diameter of the hot-wire sensor   |
| $U_{o,b}$       | bulk mean velocity  |
| $U_{o,c}$       | exit centerline mean velocity   |
| $U_c$           | local centerline mean velocity  |
| $U_{m,c}$       | centerline mean velocity maximum  |
| $U_{ic,m}$      | centerline instantaneous velocity maximum   |
| $U$             | mean velocity along lateral ( $y$ ) direction   |
| $U_i$           | instantaneous velocity  |
| $U_n$           | normalized mean velocity, where $U_n = U/U_c$   |
| $U_{n,c}$       | normalized centerline mean velocity, where $U_{n,c} = U_c/U_{o,c}$                          |
| $U_{co}$        | co-flow mean velocity   |
| $Re$            | Reynolds number defined by $Re = U_{o,c} H / \nu$   |
| $u$             | fluctuating component in the streamwise ( $x$ ) direction, $u = U_i - U_c$                  |
| $u'$            | root-mean-square (rms) of $u$ , such that $u' = (\langle u^2 \rangle)^{1/2}$                |
| $u'_c$          | centerline rms, such that $u'_c = (\langle u_c^2 \rangle)^{1/2}$                            |
| $u'_n$          | normalized rms (turbulence intensity), where $u'_n = u'/U_c$                                |
| $u'_{n,c}$      | normalized centerline rms, (centerline turbulence intensity), where $u'_{n,c} = u'_c/U_c$   |
| $u'_{c,\infty}$ | asymptotic value of centerline turbulence intensity   |
| $u'_{c,max}$    | magnitude of the local maximum of turbulence intensity                                      |
| $S_u$           | centerline skewness factor, where $S_u = \langle u^3 \rangle / (\langle u^2 \rangle)^{3/2}$ |
| $F_u$           | centerline flatness factor, where $F_u = \langle u^4 \rangle / (\langle u^2 \rangle)^2$     |



|                  |   |
|------------------|---|
| $S_u^{c,\infty}$ | asymptotic value of centerline skewness factor  |
| $S_u^{min}$      | minimum value of centerline skewness factor   |
| $S_u^{max}$      | maximum value of centerline skewness factor   |
| $F_u^{c,\infty}$ | asymptotic value of centerline flatness factor  |
| $F_u^{min}$      | minimum value of centerline flatness factor   |
| $F_u^{max}$      | maximum value of centerline flatness factor   |
| $x_p$            | jet potential core length   |
| $y_{0.5}$        | velocity half-width of the jet, i.e. the $y$ -location from the centerline, where $U = \frac{1}{2}U_c$                    |
| $K_u$            | decay rate of normalized centerline mean velocity   |
| $K_y$            | jet spreading rate  |
| $d$              | internal diameter of a round nozzle   |
| $x_{01}$         | virtual origin from the normalized mean centerline velocity   |
| $x_{02}$         | virtual origin from the normalized velocity half-widths   |
| $x_m$            | downstream distance at which a hump in turbulence intensity occurs  |
| $x_{m,\infty}$   | downstream distance at which the asymptotic value of turbulence intensity occurs  |
| $x_{p, \max}$    | maximum downstream distance up to which the flow is planar  |
| $y'_{05}/w$      | characteristic jet aspect ratio, where $y'_{0.5}$ is the velocity-half widths at $x_{p, \max}$ .                          |
| $R_o$            | adjustable overheat resistance of the CTA   |
| $R_T$            | total resistance of the sensor and cables   |
| $A_R$            | laboratory room area in the same plane as the nozzle opening width $H$  |
| $A_n$            | nozzle area   |
| $H_R$            | height of room  |
| $H_j$            | height from the bottom of room up to the nozzle   |
| $\Delta T$       | time constant of the CTA system   |
| $f_c$            | optimum cut-off frequency of the CTA system   |
| $v$              | fluctuating component in the spanwise ( $y$ ) direction, $v = V_i - V_c$  |
| $w$              | fluctuating component in the transverse ( $z$ ) direction, $w = W_i - W_c$  |
| $q$              | turbulence kinetic energy, defined by $q = \frac{1}{2}(u^2 + v^2 + w^2)$  |
| $q_{c,\infty}$   | far-field turbulent kinetic energy  |
| $St_H$           | Strouhal number for a plane jet, defined by $St_H = f H/U_{o,b}$  |
| $St_p$           | Strouhal number for a round jet, defined by $St_p = f_p D/U_{o,b}$  |
| $m$              | mass flux at any axial distance downstream from the nozzle exit   |
| $D$              | geometric diameter of a round nozzle  |
| $D_e$            | equivalent diameter of a round nozzle with the same exit area as a rectangular nozzle, where $D_e \simeq 1.13 AR^{0.5} H$ |

## 0.2 Greek Symbols

|            |   |
|------------|---|
| $\nu$      | kinematic viscosity of air, $\nu \simeq 1.47 \times 10^{-5} \text{ m}^2\text{s}^{-1}$ at 25° ambient conditions |
| $\alpha$   | overheat ratio of CTA system, usually $\simeq 1.8$  |
| $\delta$   | thickness of the boundary layer at the nozzle lip, $\delta \simeq \int_{y=0}^{y=\infty} (1 - U/U_{o,c}) dy$     |
| $\phi_u$   | power spectrum of $u$ where $\int \phi_u(f) df = \overline{u^2}$  |
| $\epsilon$ | kinetic energy dissipation term, $\epsilon \simeq 15\nu \langle (du/dx)^2 \rangle$                              |
| $\tau_w$   | viscous stress term, $(\tau_w = \rho\nu \frac{\partial U}{\partial y})$   |
| $\rho$     | density of test medium, for air $\rho \simeq 1.2 \text{ kg m}^{-3}$ at 25° ambient conditions                   |

## 0.3 Some Special Terms

- (1) Nozzle profile factor: denoted as  $r^*$  and defined by  $r/H$ .
- (2) Plane jet: a jet which issues through a rectangular nozzle with sidewalls.
- (3) Quasi-plane jet: a jet which issues through a large aspect ratio rectangular nozzle but no sidewalls.
- (4) Round jet: a jet that issues through a round nozzle.
- (5) Pipe jet: a jet through a long pipe.

## 0.4 Coordinate System

|     |                                 |
|-----|---------------------------------|
| $x$ | axial (streamwise) coordinate   |
| $y$ | lateral (transverse) coordinate |
| $z$ | spanwise coordinate             |

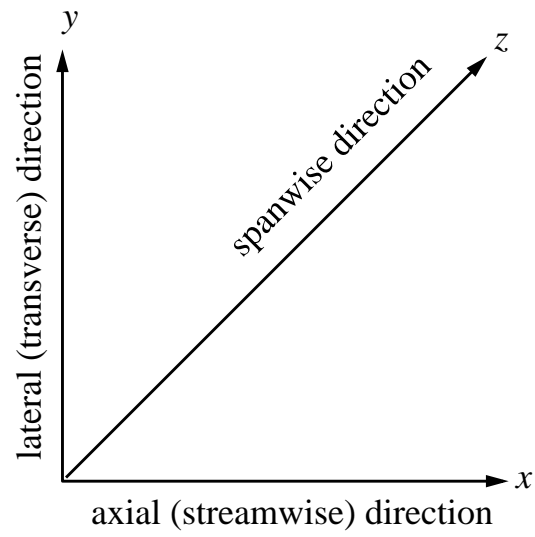


Figure 1: The coordinate system used in the present study.